Cancer Microenvironment (2013) 6:247–261
DOI 10.1007/s12307-013-0132-4

ORIGINAL PAPER

Gene Expression Profiling Reveals Regulation of ERK Phosphorylation by Androgen-Induced Tumor Suppressor U19/EAF2 in the Mouse Prostate

Fei Su · Bruna R. S. Correa · Jianhua Luo · Ricardo Z. N. Vencio · Laura E. Pascal · Zhou Wang

Received: 26 November 2012 / Accepted: 12 February 2013 / Published online: 26 February 2013
© Springer Science+Business Media Dordrecht 2013

Abstract *U19/EAF2* is regulated by androgens in the prostate and capable of regulating transcriptional elongation of RNA *Pol* II via interaction with the ELL family proteins. Inactivation of *U19/EAF2* induces tumorigenesis in multiple organs; however the mechanism of *U19/EAF2* tumor suppression remains unclear. To elucidate potential mechanisms of U19/EAF2 action, we performed cDNA microarray analysis and identified 164 mRNA transcripts regulated by U19/EAF2 in the mouse ventral prostate. Bioinformatics analysis indicated that U19/EAF2 knockout activates the RAS-BRAF-ERK signaling pathway, which is known to play important roles in carcinogenesis. qPCR verified increased expression of BRAF mRNA, and immunostaining and Western blot analysis demonstrated increased expression of p-ERK at the protein level suggested U19/EAF2 knockout activates this important pathway. These findings indicate that loss of EAF2 up-regulates transcription of RAS cascade genes including Grb2, PI3K, and BRAF, leading to elevated p-ERK levels, which may represent a major functional role of U19/EAF2 in the prostate. Furthermore, these observations suggest that U19/EAF2 is a key player in crosstalk between androgen receptor and the RAS-BRAF-ERK signaling pathway.

Keywords EAF2 · Prostate cancer · ERK

Electronic supplementary material The online version of this article (doi:10.1007/s12307-013-0132-4) contains supplementary material, which is available to authorized users.

F. Su · L. E. Pascal · Z. Wang
Department of Urology, University of Pittsburgh, Pittsburgh, PA 15232, USA

J. Luo
Department of Pathology, University of Pittsburgh, Pittsburgh, PA 15232, USA

Z. Wang
Department of Pharmacology and Chemical Biology, University of Pittsburgh, Pittsburgh, PA 15232, USA

B. R. S. Correa · R. Z. N. Vencio
Department of Computing and Mathematics FFCLRP-USP, University of São Paulo, Ribeirão Preto, Brazil

Z. Wang (✉)
Department of Urology, University of Pittsburgh Cancer Institute, 5200 Centre Ave, Suite G40, Pittsburgh, PA 15232, USA
e-mail: wangz2@upmc.edu

Present Address:
F. Su
Center for Nuclear Receptors and Cell Signaling, University of Houston, Houston, TX 77204, USA

Introduction

Androgens play a key role in prostate development, maturation, homeostasis, and pathogenesis including benign prostatic hyperplasia (BPH) and prostate cancer [1–4]. Androgen action is mediated through the androgen receptor (AR), a ligand-regulated transcription factor that regulates the expression of many androgen-responsive genes [5, 6]. Defining the functions of various androgen-responsive genes will provide insights into the mechanisms of androgen action in the prostate.

Androgen action in the prostate, particularly in the regulation of prostate homeostasis, is likely to involve crosstalk with various growth signaling, including the EGF, IGF, TGF-β, FGF, and VEGF signaling pathways [7, 8]. Many experiments demonstrating crosstalk between AR and various signaling pathways have been carried out in prostate cancer cells. The importance of crosstalk in the normal prostate is less clear. Defining AR crosstalk with important

signaling pathways in the mouse prostate will provide new insights into the mechanisms by which androgens regulate prostate growth, regression, and homeostasis under physiological conditions.

One important growth signal pathway is the RAS-BRAF-MEK-ERK cascade, which is frequently activated in carcinogenesis [9]. Activation of ERK via phosphorylation is a critical step in tumor development and maintenance. The RAS-ERK pathway is exquisitely sensitive to small changes in the levels of or activity of BRAF and BRAF may be the primary target of oncogenic RAS [10]. The BRAF gene encodes a protein belonging to the raf/mil family of serine/threonine protein kinases and plays a role in regulating the MAP kinase/ERKs signaling pathway, which affects cell division, differentiation, and secretion. In humans, activating oncogenic mutations in this gene have also been associated with development of the cardio-facio-cutaneous (CFC) syndrome [11] and various cancers, most frequently in melanoma, papillary thyroid cancer and colon cancer [12–16]. Elevated ERK signaling has been found in prostate cancer patients [7, 17–19]. Sorafenib, an inhibitor of human BRAF protein [20], is in Phase II clinical trial in androgen-independent prostate cancer [21].

Our previous studies showed that androgen-responsive gene (Up-regulated gene 19/ELL associated factor 2) U19/EAF2 encodes a potential tumor suppressor. U19/EAF2 expression is frequently down-regulated in advanced human prostate cancer specimens as well as in established prostate cancer cell lines [22]. U19/EAF2, along with its homolog EAF1, has been reported to regulate transcriptional elongation of RNA polymerae II via interaction with the ELL (11 lysine-rich leukemia) family proteins [23–25]. Overexpression of *U19/EAF2* induces apoptosis and suppresses prostate xenograft tumor growth [22]. Inactivation of *U19/EAF2* in a murine knockout model leads to high rates of lung adenocarcinoma, B cell lymphoma, hepatocellular carcinoma, and prostate intraepithelial neoplasia (PIN) [26]. The U19/EAF2 KO prostate exhibited epithelial hyperplasia and dysplasia, suggesting that *U19/EAF2* contributes to the suppression of prostate tumors. The mechanisms of *U19/EAF2* acting as a novel tumor suppressor in multiple mouse tissues are not clear.

Our previous studies showed that U19/EAF2 knockout prostate exhibited elevated cell proliferation, suggesting a possible link between U19/EAF2 with growth control signaling pathways [26]. Identification of signaling pathways regulated by U19/EAF2 in the mouse prostate model would suggest potential mechanisms of U19/EAF2 action and provide further insights into androgen action in the prostate.

Using cDNA microarray, this study identified 49 up-regulated and 115 down-regulated genes in the U19/EAF2 knockout prostate as compared to wild-type controls. Bioinformatics analysis of these differentially regulated genes revealed multiple pathways that are regulated by U19/EAF2 in the prostate. Loss of EAF2 in the murine prostate induced an up-regulation of RAS cascade genes including Grb2, PI3K, and BRAF, leading to elevated p-ERK levels, which may represent a major mechanism by which U19/EAF2 down-regulation induces prostate tumorigenesis.

Materials and Methods

Animals

We previously generated *U19/EAF2* heterozygous mice (*U19/EAF2* $^{+/-}$) using HM1 embryonic stem cells [26]. Briefly, heterozygous mice were thereafter backcrossed to the C57BL/6J strain (The Jackson Laboratory, Bar Harbor, ME) for more than 12 generations to generate *U19/EAF2* knockout (KO) mice with a pure C57BL/6J background under approval by the Institutional Animal Care and Use Committee of the University of Pittsburgh. Genotyping was determined by PCR analysis of mouse tail genomic DNA as described previously [26].

Tissue Preparation and Microarray Hybridization

Ventral prostate lobes (VP) from 3 month old wild-type (WT) and *U19/EAF2* KO virgin male mice were microdissected from the anterior (AP), dorsal (DP), and lateral (DL) lobes in phosphate-buffered saline with the aid of a dissecting Carl Zeiss Stemi 2000 Steromicroscope (Zeiss) and immediately snap-frozen in liquid nitrogen. Five lobes of each type from the same mouse strain were pooled in order to minimize individual differences. Expression profiling experiments were performed by the Microarray Laboratory at University of Pittsburgh. Microarray hybridization was performed with a pre-equilibrated Mouse Genome 430 2.0 Genechip array (Affymetrix Inc., Santa Clara, CA). In addition, to compensate for the extremely small sample setup (n=1, with pooling of five animals), we performed 6 independent biological replicates of individual ventral lobes from wild type mice and accessed their gene expression using the Illumina Mouse-48 K Expression BeadChip (Illumina, San Diego, CA). All datasets have been deposited in the NCBI public database GEO with the following accession number: GSE34511.

Bioinformatics Data Analysis

Probe intensities too low to be considered as present were filtered out using the long established Affymetrix default methods. Probes presenting detection p-values smaller than 0.01 were further considered in knockout (KO) vs wild type

(WT) gene expression comparison. Differential expression statistical significance was obtained with the HTself2 method [27] which uses self-self experiments to extrapolate *p*-values for small sample sized experiments. Small modifications to the HTself2 methods were introduced to make it suitable for single-color microarray data. In order to facilitate reuse and detailed methodological reproducibility and understanding, the analysis script written in the R statistical language (R Development Core Team, 2011) is freely available with no usage restriction at: http://labpib.fmrp.usp.br/~rvencio/htself2/. The whole filtered average log intensity range was used to establish the null probability density distribution considering virtual self-self experiments generated from every possible combination among 6 wild type mice expression data similarly as in previous works [28–30]. A Bonferroni-corrected *p*-value of 0.01 was used as statistical significance threshold, which was found to correspond to a 2.5-fold change cutoff. Functional enrichment analysis was performed with DAVID (http://david.abcc.ncifcrf.gov/) as described in Huang et al. [31]. Functional and ontology enrichment analysis was performed using the DAVID web-based tool [32] and Ingenuity Pathways Analysis (IPA) 5.0 (Ingenuity Systems).

Gene Expression Validation

In addition to the samples used in microarray analysis, the ventral prostates and livers of an independent set of wild-type or *U19/EAF2* knockout male mice (n=3) at 3 months of age were used for total RNA isolation using Trizol® Reagent (Invitrogen, USA). Animal tissues were homogenized with a Kontes pellet pestle for 30 s twice (Fisher Scientific, Fair View, NJ). qPCR verified expression scored by cDNA arrays of ventral prostate tissue and expression levels in liver tissue (Platinum SYBR®Green qPCR SuperMix-UDG, Invitrogen, USA). PCR amplification was carried out using Applied Biosystems StepOne™Plus™ Real-Time PCR Systems (Applied Biosystems CA, USA). PCR amplification of various genes was normalized to the average Ct value of the housekeeping gene GAPDH. Primer sequences are listed in Table 1. GAPDH was chosen as an internal control because there was no difference in GAPDH expression between wild-type and U19/EAF2 knockout prostate in the microarray data. Also GAPDH has been used as a normalization control in prostate research [33]. Each experimental sample was assayed in triplicate.

Western Blot of Mouse Tissue

Protein lysates were obtained from freshly isolated individual mouse liver and prostate tissues. Animal tissues were homogenized by a hand homogenizer, Kontes® Pellet Pestle®/Cordless Motor (Fisher, USA) in RIPA lysis buffer (50 mM Tris–HCl, pH8.0, 150 mMNaCl, 1 mM EDTA, 1 % (v/v) NP-40, 0.1 % SDS, 0.25 % sodium deoxycholate, 1 mM sodium orthovanadate, 1 mM PMSF, 1:100 dilution of protease inhibitor cocktail (P8340, Sigma-Aldrich, St. Louis, MO). Protein concentration was determined by BCA Protein Assay (Thermo Scientific, Rockford, IL). The whole cell lysate (WCL) (45 ug/lane) were boiled in SDS sample buffer, separated on a NEXT GEL™ 10 % (Amresco) under reducing conditions, and then transferred onto a nitrocellulose membrane. Blotted proteins were probed with antibodies as follows: Phospho-p44/42 MAPK (Erk1/2) (Thr202/Tyr204) antibody (1:1000, #9101), p44/42 MAPK (Erk1/2) antibody (1:1000, #9102, Cell Signaling Technology) and followed with HRP (Horseradish peroxidase) labeled secondary antibodies (Santa Cruz Biotechnology). Signals were visualized using chemiluminescence (ECL™ Western Blotting Detection Reagents®, GE Healthcare) and were exposed to X-ray film (Fuji film).

Immunohistochemical Analyses

Tissue specimens from 3 month-old male mice were frozen in OCT (Tissue Tek, Sakura Finetechnical USA, Torrance, CA) immediately after dissection and stored at −80 °C. Serial 5 μm sections were fixed in cold acetone and processed for immunohistochemistry. Sections were incubated with rabbit polyclonal Phospho-p44/42 MAPK (Erk1/2) (Thr202/Tyr204) antibody (1:1000, #9101, Cell Signaling Technology) or rabbit polyclonal p44/42 MAPK (Erk1/2) antibody (1:1000, #9102, Cell Signaling Technology) at room temperature for 1 h. Antigen was localized using HRP-conjugated anti- rabbit IgG (Santa Cruz Biotechnology) as the secondary antibody and diaminobenzidine tetrahydrochloride as the chromagen. Negative control experiments were performed using goat or rat IgG as primary antibody. The sections were lightly counterstained with hematoxylin.

Statistical Analysis

All values represent the mean ± standard error of the mean (SEM). Statistical significance between paired data was assessed by unpaired Student's t test and any p-value less than 0.05 was considered statistically significant.

Results

Microarray Analysis of Genes Differentially Expressed in the Ventral Prostate of U19/EAF2 Knockout Mouse

To identify target genes of U19/EAF2, we performed cDNA microarray analysis of the ventral prostate from wild-type and

Table 1 The list of genes and primer sequences used for RT-PCR analysis

ID	Symbol	Entrez gene name	Direction	Sequence
1422651_at	Adipoq	adiponectin, C1Q and collagen domain containing	Forward	5′- TGTTCCTCTTAATCCTGCCCA
			Reverse	5′- CCA ACC TGC ACA AGT TCC CTT
1428944_at	Ube1l2	ubiquitin-like modifier activating enzyme 6	Forward	5′- GAG CCT GCG GTG CAA GTA A
			Reverse	5′- CCA CTC CAA GAC CAC CCA TAC
1425032_at	Abpb	androgen binding protein beta	Forward	5′- GCA TGT GCT CCT TTT GTC GG
			Reverse	5′- TGG TTC CTC ATT GAA GCA ATC C
1419554_at	CD47	CD47 antigen	Forward	5′- TGC GGT TCA GCT CAA CTA CTG
			Reverse	5′- GCT TTG CGC CTC CAC ATT AC
1449676_at	Rab2	RAB2A, member RAS oncogene family	Forward	5′- GCG ACA CAG GTG TTG GTA AAT
			Reverse	5′- CAT CAA TCG TTA TCA TCC GAG CA
1449028_at	Rhou	ras homolog gene family, member U	Forward	5′- GGC TAC CCC ACC GAG TAC AT
			Reverse	5′- GGG GCC TCA GCT TGT CAA A
1435831_at	UPK IB	uroplakin 1B	Forward	5′- CAC TGT TCG TTG CTT CCA GG
			Reverse	5′- GCT TCG AGA AGT GGG TAA AGA CT
1450849_at	hnRNP	heterogeneous nuclear ribonucleoprotein U	Forward	ATG AGT TCT TCG CCT GTT AAT GT
			Reverse	5′- CCT GGA GTC GAT CCA TGA GA
1449405_at	Tensin	tensin 1	Forward	5′- GTT TCT CCA AGC ATA CAG CCA
			Reverse	5′- GTT CAG AGA GGT TGA ATA GCA GG
1460302_at	THBS1	thrombospondin 1	Forward	5′- GGG GAG ATA ACG GTG TGT TTG
			Reverse	5′- CGG GGA TCA GGT TGG CAT
1448556_at	PRLR	prolactin receptor	Forward	5′- GGG GAG ATA ACG GTG TGT TTG
			Reverse	5′- CGG GGA TCA GGT TGG CAT
M32599	GAPDH	glyceraldehyde-3-phosphate dehydrogenase	Forward	5′-AGG TCG GTG TGA ACG GAT TTG
			Reverse	5′-GTA GAC CAT GTA GTT GAG GTC A

U19/EAF2 knockout mice at 3 months of age. On a C57BL/6J background, U19/EAF2 knockout mice displayed no histological abnormality in the prostate at this age (Ai et al., in revision). Thus, all changes are unlikely to be secondary to pathological changes in the knockout prostate. Due to an extremely small sample setup (n=1, pooled from five animals), appropriate bioinformatics strategies were necessary. Methods to deal with such special situations exist and we used the HTself2 method [27] with small modifications. The idea behind this method is to guide fold-change cutoff selection, an arbitrary, but necessary, step to define the differentially expressed genes, with experimental data that estimates the natural inter-mice genetic noise in gene expression measurements. In order to estimate this background noise we performed six independent biological replicates of wild type (WT) mice and assessed their gene expression. Although the statistical method was originally designed for ratio-based two-color microarray, we adapted our results to take advantage of it by simply creating virtual experiments taking all possible combinations from the 6 WT expression profiles (WT_1 vs WT_2, WT_1 vs WT_3, …, WT_6 vs WT_5) similarly as carried out in Pascal et al. [26–28]. The probability density distribution of the log fold-change obtained with this strategy can then be used to derive a statistically consistent cutoff criteria for differential expression finding in the knockout vs wild type experiment (KO/WT) (Fig. 1a). In small sample scenarios it is important to be overly conservative, therefore, the significance figures (p-values) found with the modified Cortez et al. [23] method were also corrected for multiple testing issues with the highly stringent Bonferroni correction [34] (Fig. 1b). We found that a 2.5-fold change cutoff corresponded to Bonferroni-corrected p-values of less than 0.01 so this threshold was applied to define up-regulated (KO/WT>2.5) and down-regulated (KO/WT<1/2.5) genes (Fig. 1c, Table 2).

Several genes identified as down-regulated in the U19/EAF2 murine prostate have been reported to play roles in the extracellular matrix of the tumor microenvironment, notably a 2.5-fold decrease in a disintegrin and metallopeptidase domain 28 (ADAM28), a 7.3-fold decrease in bromodomain containg 4 (BRD4), a 2.7-fold decrease in occludin (OCLN) and a 2.6-fold decrease in collagen IV (COL4A2). ADAM28 can bind to the integrin $\alpha 4\beta 1$, suggesting a potential adhesive and proteolytic role inflammatory and immune processes [35]. The bromodomain containing 4 (BRD4) gene has been shown to regulate the expression extra-cellular matrix-related genes and inhibit metastasis in breast cancer [36]. Occludin is a tight junction protein that has been associated with loss of polarity

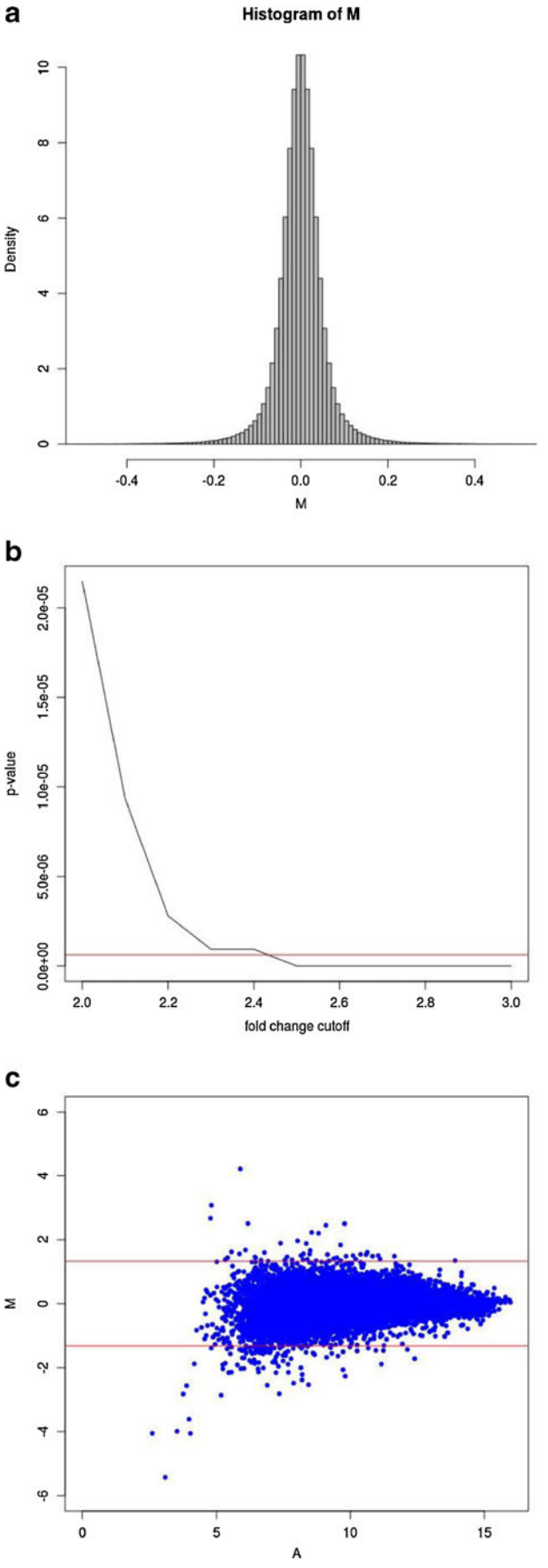

Fig. 1 HTself2 analysis of microarray data. **a**. Self-self empirical probability density distribution. Virtual log ratios (M) where derived from all possible pairwise combinations among 6 independent wild type experiments analyzing gene expression in the ventral prostate at age 3 month. Fold-changes greater than 2-fold (M>1 or M<−1) have a very small probability of happening (<0.0001) due by chance alone considering the intrinsic inter-animal genetic noise. **b**. Interchange between statistical significance and fold-chance cutoffs. Statistical significance thresholds (*p*-value) can be mapped directly to equivalent fold-change cutoffs to define differentially expressed genes in the knockout vs wild type experiment. The horizontal red line represents a traditional 0.01 significance cutoff after multiple testing correction by the stringent Bonferroni method. A 2.5-fold change cutoff criteria would be equivalent to a corrected p-value smaller than 0.01. **c**. MA-plot showing the knockout (KO) vs wild type (WT) experiment. Virtual log ratios (M) remain stable around zero (KO/WT=1) along all average log intensity (A) scale. Horizontal red lines represent fold-change cutoffs (KO/WT>2.5-fold or KO/WT<1/2.5) presenting multiple testing adjusted *p*-values<0.01 and, therefore, define the differentially expressed genes

in prostate cancer cells [37]. Collagen IV is the major component of the basement membrane and the C-terminal portion of the protein, known as canstatin, is an inhibitor of angiogenesis and tumor growth [38]. Disrupted EAF2 regulation of these genes could promote changes in the extracellular matrix thereby contributing to prostate tumor development and progression.

qPCR in a different set of WT and KO mice (n=3) at 3 months of age was used to validate that genes identified by cDNA microarray were indeed up- or down-regulated by U19/EAF2 knockout in the mouse prostate. The following genes: Adipoq (* p=0.006), Ube1l2 (* p=0.01), Abpb (* p=0.01), CD47 (* p=0.006), Rab2 (* p=0.04), Rhou (* p=0.05), Uroplakin iB (* p=0.01), hnRNP (* p=0.02), PRLR (* p=0.05), Tesin (* p=0.03), and Thbs1 (* p=0.0004) were chosen randomly or because they encode products that are important in tumorigenesis for qPCR analysis, and p values were determined by comparing the U19/EAF2 knockout with wild-type (Fig. 2a). Fold changes from the microarray platforms were plotted versus the corresponding fold changes from qPCR (Fig. 2b), and Pearson correlation coefficient between microarray and qPCR results was 0.92, indicating high concordance among these independent biological replicates.

Gene Ontology and KEGG Pathway Analysis of U19/EAF2 Downstream Genes

The known functional classification of differentially expressed genes was analyzed for significant enrichment with respect to various functional categories using the DAVID annotation tool [32] (http://david.abcc.ncifcrf.gov/), which examines all the functions represented by each gene in a list of genes and identifies groups that are functionally related. The over-represented ontology-based classification groups form the basis for identifying functional processes represented in the change of state induced by *U19/EAF2* loss. The major biological themes among the up-regulated and down-regulated genes are

Table 2 Differentially expressed genes in wild-type and *U19/EAF2* knockout ventral prostate

ID	WT intensity	KO intensity	log2 (KO/WT)	Fold-change KO vs WT	Diff expr	Gene name
1416497_at	1364.2	3584.2	1.39	2.6	KO > WT	protein disulfide isomerase associated 4
1417225_at	913.2	2773.2	1.6	3	KO > WT	ADP-ribosylation factor-like 6 interacting protein 5
1417594_at	333.9	967.7	1.54	2.9	KO > WT	G kinase anchoring protein 1
1417867_at	170.9	629.2	1.88	3.7	KO > WT	complement factor D (adipsin)
1418666_at	33.9	99.6	1.55	2.9	KO > WT	pentraxin related gene
1419554_at	372.1	939.8	1.34	2.5	KO > WT	CD47 antigen (Rh-related antigen, integrin-associated signal transducer)
1419946_s_at	408.9	1083.9	1.41	2.7	KO > WT	predicted gene 5865; RAB2A, member RAS oncogene family
1420037_at	780.4	2270.4	1.54	2.9	KO > WT	ATP synthase, H+ transporting, mitochondrial F1 complex, alpha subunit, isoform 1
1420125_at	30.3	172	2.51	5.7	KO > WT	T-cell leukemia translocation altered gene
1421163_a_at	371.3	2100.2	2.5	5.7	KO > WT	nuclear factor I/A
1421636_at	37.8	120.8	1.68	3.2	KO > WT	TBC1 domain family, member 8B
1422142_at	141.5	365.9	1.37	2.6	KO > WT	nephrosis 1 homolog, nephrin (human)
1422651_at	13.8	255.5	4.21	19	KO > WT	adiponectin, C1Q and collagen domain containing
1423420_at	25	64.8	1.37	2.6	KO > WT	adrenergic receptor, beta 1
1424101_at	503.7	1278.3	1.34	2.5	KO > WT	heterogeneous nuclear ribonucleoprotein L
1425032_at	653.3	1851.5	1.5	2.8	KO > WT	androgen binding protein beta
1428944_at	421.4	1505.4	1.84	3.6	KO > WT	ubiquitin-like modifier activating enzyme 6
1431638_at	53.7	145.4	1.44	2.7	KO > WT	RIKEN cDNA 4930592A05 gene
1432372_a_at	177.7	523.4	1.56	2.9	KO > WT	sepiapterin reductase
1433078_at	9.7	81.7	3.07	8.4	KO > WT	RIKEN cDNA 5830435N06 gene
1434987_at	175.1	819	2.23	4.7	KO > WT	aldehyde dehydrogenase 2, mitochondrial
1434988_x_at	204.5	647.5	1.66	3.2	KO > WT	aldehyde dehydrogenase 2, mitochondrial
1435679_at	265.9	673.9	1.34	2.5	KO > WT	optineurin
1438120_x_at	728.3	1907.3	1.39	2.6	KO > WT	interleukin-1 receptor-associated kinase 1
1438219_at	87.9	325.6	1.89	3.7	KO > WT	similar to hCG45299; purine rich element binding protein A
1438309_at	209.5	613	1.55	2.9	KO > WT	activin A receptor, type IC
1438562_a_at	1250	3547.9	1.51	2.8	KO > WT	protein tyrosine phosphatase, non-receptor type 2
1439224_at	187.2	485.4	1.37	2.6	KO > WT	ankyrin repeat and IBR domain containing 1
1439260_a_at	494.3	1256.2	1.35	2.5	KO > WT	ectonucleotide pyrophosphatase/phosphodiesterase 3
1439263_at	63.6	163.1	1.36	2.6	KO > WT	hypothetical LOC14210
1441830_x_at	10.9	69.3	2.67	6.4	KO > WT	A kinase (PRKA) anchor protein 10
1446291_at	25.9	70.1	1.44	2.7	KO > WT	RIKEN cDNA 9330175H22 gene
1447996_at	548.2	1532.2	1.48	2.8	KO > WT	expressed sequence AI848149
1448068_at	120.3	331.6	1.46	2.8	KO > WT	sterol O-acyltransferase 1
1448503_at	9654.6	24560	1.35	2.5	KO > WT	similar to myeloid cell leukemia sequence 1; myeloid cell leukemia sequence 1
1448761_a_at	438.7	1188.7	1.44	2.7	KO > WT	coatomer protein complex, subunit gamma 2
1449114_at	77.5	194.4	1.33	2.5	KO > WT	serine/threonine kinase 3 (Ste20, yeast homolog)
1449434_at	233.9	1278.2	2.45	5.5	KO > WT	carbonic anhydrase 3
1449681_at	170.2	483	1.5	2.8	KO > WT	hepatoma-derived growth factor
1450232_at	26.9	82.6	1.62	3.1	KO > WT	X-linked inhibitor of apoptosis
1451285_at	905.5	2620.4	1.53	2.9	KO > WT	fusion, derived from t(12;16) malignant liposarcoma (human)
1452124_at	1915.1	5358.9	1.48	2.8	KO > WT	ankyrin 3, epithelial

Table 2 (continued)

ID	WT intensity	KO intensity	log2 (KO/WT)	Fold-change KO vs WT	Diff expr	Gene name
1454278_at	209.1	545.3	1.38	2.6	KO > WT	RIKEN cDNA A430105D02 gene
1454634_at	64.1	194.1	1.6	3	KO > WT	fucokinase
1455381_at	210.2	965.8	2.2	4.6	KO > WT	hypothetical protein LOC100045622; RIKEN cDNA 4921513D23 gene
1456505_at	1089.1	3046.2	1.48	2.8	KO > WT	Braf transforming gene
1456843_at	133	518.9	1.96	3.9	KO > WT	Yamaguchi sarcoma viral (v-yes) oncogene homolog 1
1456961_at	117.9	302.4	1.36	2.6	KO > WT	enhancer of yellow 2 homolog (Drosophila); predicted gene 16373
1459882_at	52.3	143.9	1.46	2.8	KO > WT	ASF1 anti-silencing function 1 homolog A (S. cerevisiae)
1425191_at	210.2	79.1	−1.41	2.7	WT > KO	occludin/ELL domain containing 1
1443220_at	315.3	81.1	−1.96	3.9	WT > KO	reticulon 3
1442846_at	572.3	142.7	−2	4	WT > KO	pre B-cell leukemia transcription factor 1; region containing RIKEN cDNA 2310056B04 gene; pre B-cell leukemia transcription factor 1
1459309_at	45.4	17.3	−1.39	2.6	WT > KO	RUN and FYVE domain containing 3
1455956_x_at	189.3	72.6	−1.38	2.6	WT > KO	cyclin D2
1443077_at	401.9	121.9	−1.72	3.3	WT > KO	hypothetical protein LOC100043982; RIKEN cDNA 1700081L11 gene
1432134_at	56	1.3	−5.43	43	WT > KO	methyltransferase like 4, pseudogene 1
1446196_at	34.7	9.4	−1.88	3.7	WT > KO	predicted gene 7996; high mobility group AT-hook 2
1434497_at	166.2	59.1	−1.49	2.8	WT > KO	RIKEN cDNA 4933431E20 gene
1446149_at	260.6	73.2	−1.83	3.6	WT > KO	protein phosphatase 3, catalytic subunit, beta isoform
1435061_at	705.3	234.1	−1.59	3	WT > KO	nudix (nucleoside diphosphate linked moiety X)-type motif 11; nudix (nucleoside diphosphate linked moiety X)-type motif 10
1427217_at	69	25.9	−1.41	2.7	WT > KO	zinc finger protein 455
1435415_x_at	117.5	36.3	−1.69	3.2	WT > KO	MARCKS-like 1; predicted gene 9106
1441724_at	283.7	113.3	−1.32	2.5	WT > KO	stromal antigen 1
1459398_at	231.8	88.3	−1.39	2.6	WT > KO	pellino 1
1433288_at	76.7	18.7	−2.04	4.1	WT > KO	RIKEN cDNA 1520401O13 gene
1435831_at	1969	408.8	−2.27	4.8	WT > KO	uroplakin 1B
1455464_x_at	1735.9	415.6	−2.06	4.2	WT > KO	uroplakin 1B
1428492_at	155.5	46.1	−1.75	3.4	WT > KO	GLI pathogenesis-related 2
1433944_at	111.9	40.4	−1.47	2.8	WT > KO	HECT domain containing 2
1457348_at	1313.1	421.5	−1.64	3.1	WT > KO	ADP-ribosylation factor 4
1440314_at	474.4	187.7	−1.34	2.5	WT > KO	thyroid hormone receptor interactor 12
1444125_at	434.2	61.7	−2.82	7	WT > KO	BEN domain containing 6
1455164_at	560	100.1	−2.48	5.6	WT > KO	CDC42 GTPase-activating protein
1450849_at	7353.3	2719.9	−1.43	2.7	WT > KO	heterogeneous nuclear ribonucleoprotein U
1456834_at	102.5	37.2	−1.46	2.8	WT > KO	ring finger protein 144B
1450457_at	282.9	78.7	−1.85	3.6	WT > KO	similar to Casitas B-lineage lymphoma; Casitas B-lineage lymphoma
1444951_at	552.5	192.7	−1.52	2.9	WT > KO	DENN/MADD domain containing 1B
1456078_x_at	267	84.4	−1.66	3.2	WT > KO	tubulin, beta 2c, psuedogene 1; tubulin, beta 2C; tubulin, beta 2c, pseudogene 2
1458666_at	200	45.5	−2.14	4.4	WT > KO	Rho GTPase activating protein 1; predicted gene 8514

Table 2 (continued)

ID	WT intensity	KO intensity	log2 (KO/WT)	Fold-change KO vs WT	Diff expr	Gene name
1417055_at	4404.3	1187.6	−1.89	3.7	WT > KO	RIKEN cDNA 0610009D07 gene
1455986_at	73	19.4	−1.91	3.8	WT > KO	zinc finger, DHHC domain containing 17
1460066_at	993.6	310.5	−1.68	3.2	WT > KO	expressed sequence C80889
1434730_at	122	47.3	−1.37	2.6	WT > KO	expressed sequence AI854517
1452284_at	155.3	54.9	−1.5	2.8	WT > KO	protein tyrosine phosphatase, receptor type Z, polypeptide 1
1460336_at	635.5	136.9	−2.21	4.6	WT > KO	peroxisome proliferative activated receptor, gamma, coactivator 1 alpha
1439902_at	66.5	4	−4.06	17	WT > KO	complement component 5a receptor 1
1444692_at	98.9	22.4	−2.14	4.4	WT > KO	EST AI316844
1457618_at	337.2	109.6	−1.62	3.1	WT > KO	DEAD (Asp-Glu-Ala-Asp) box polypeptide 6
1452027_a_at	129.4	46.1	−1.49	2.8	WT > KO	transformation related protein 63
1430464_at	131.5	32.3	−2.03	4.1	WT > KO	RIKEN cDNA 9430021M05 gene
1430472_at	36.1	5.1	−2.82	7.1	WT > KO	armadillo repeat containing 1
1442918_at	190.5	46.5	−2.03	4.1	WT > KO	neuron navigator 3
1424051_at	471.4	178.8	−1.4	2.6	WT > KO	collagen, type IV, alpha 2
1460427_a_at	261.3	103.7	−1.33	2.5	WT > KO	a disintegrin and metallopeptidase domain 28
1436968_x_at	990.6	381.6	−1.38	2.6	WT > KO	kelch-like 24 (Drosophila)
1457343_at	315.3	102.7	−1.62	3.1	WT > KO	adaptor-related protein complex AP-4, sigma 1
1447402_at	168.9	58.1	−1.54	2.9	WT > KO	ataxin 1
1445066_at	121.8	29.8	−2.03	4.1	WT > KO	tetratricopeptide repeat domain 7B
1441579_at	36	6.1	−2.56	5.9	WT > KO	doublesex and mab-3 related transcription factor like family A1
1435529_at	217.8	75.3	−1.53	2.9	WT > KO	predicted gene 14446
1437311_at	1432.7	504.2	−1.51	2.8	WT > KO	small nucleolar RNA host gene 11 (non-protein coding)
1449318_at	181.9	50.7	−1.84	3.6	WT > KO	similar to Tubulin, gamma 2; tubulin, gamma 2
1436981_a_at	9813.1	2978.1	−1.72	3.3	WT > KO	tyrosine 3-monooxygenase/tryptophan 5-monooxygenase activation protein, zeta polypeptide; predicted gene 4202
1448359_a_at	161.8	63	−1.36	2.6	WT > KO	HIG1 domain family, member 1A
1458700_at	170.8	60.9	−1.49	2.8	WT > KO	leucine rich repeat containing 8 family, member C
1447905_x_at	2642.3	1006.4	−1.39	2.6	WT > KO	nucleoporin 62
1442867_at	335.6	97.1	−1.79	3.5	WT > KO	multiple EGF-like-domains 11
1421868_a_at	146.1	56.3	−1.38	2.6	WT > KO	pancreatic lipase
1443441_x_at	110.9	42.9	−1.37	2.6	WT > KO	predicted gene 5141
1439847_s_at	149.5	41.9	−1.84	3.6	WT > KO	Kruppel-like factor 12
1441764_at	144.8	57	−1.35	2.5	WT > KO	PR domain containing 10
1459104_at	175.5	69.6	−1.33	2.5	WT > KO	budding uninhibited by benzimidazoles 3 homolog (S. cerevisiae)
1446736_at	184.9	62.2	−1.57	3	WT > KO	MyoD family inhibitor domain containing
1440716_at	106.7	28.3	−1.91	3.8	WT > KO	RIKEN cDNA 6430604M11 gene
1453593_at	183.5	70.2	−1.39	2.6	WT > KO	vestigial like 3 (Drosophila)
1446421_at	151.7	57.6	−1.4	2.6	WT > KO	schwannomin interacting protein 1
1433183_at	24.9	1.5	−4.05	17	WT > KO	RIKEN cDNA 6720477C19 gene
1426095_a_at	270.4	103	−1.39	2.6	WT > KO	tumor necrosis factor receptor superfamily, member 22
1431079_at	172.2	64.3	−1.42	2.7	WT > KO	C1q and tumor necrosis factor related protein 2
1424507_at	77	21.1	−1.87	3.6	WT > KO	Ras and Rab interactor 1

Table 2 (continued)

ID	WT intensity	KO intensity	log2 (KO/WT)	Fold-change KO vs WT	Diff expr	Gene name
1421603_a_at	395.1	106.3	−1.89	3.7	WT > KO	carcinoembryonic antigen-related cell adhesion molecule 1; carcinoembryonic antigen-related cell adhesion molecule 2
1451870_a_at	117.7	40.1	−1.55	2.9	WT > KO	bromodomain containing 4
1431306_at	97.5	13.4	−2.86	7.3	WT > KO	5′-nucleotidase, cytosolic III
1436713_s_at	78.8	26.6	−1.57	3	WT > KO	maternally expressed 3
1441701_at	326.4	107.2	−1.61	3	WT > KO	zinc finger protein 148
1443447_at	133.9	52.5	−1.35	2.6	WT > KO	5-azacytidine induced gene 2
1453371_at	438.4	174.5	−1.33	2.5	WT > KO	regulation of nuclear pre-mRNA domain containing 2
1429882_at	1621.2	632.3	−1.36	2.6	WT > KO	RIKEN cDNA 6820431F20 gene
1445530_at	46.1	2.9	−3.99	16	WT > KO	transmembrane protein 194B
1444279_at	668.1	229.4	−1.54	2.9	WT > KO	HECT, UBA and WWE domain containing 1
1458832_at	176	68.7	−1.36	2.6	WT > KO	growth hormone receptor
1452517_at	1086.2	369.7	−1.55	2.9	WT > KO	pleckstrin homology domain containing, family H (with MyTH4 domain) member 1
1425847_a_at	148.2	51.1	−1.54	2.9	WT > KO	RIKEN cDNA B230120H23 gene
1438662_at	93.1	20.9	−2.16	4.5	WT > KO	adherens junction associated protein 1
1425934_a_at	671.3	128.8	−2.38	5.2	WT > KO	UDP-Gal:betaGlcNAc beta 1,4-galactosyltransferase, polypeptide 4
1422140_at	163	46.2	−1.82	3.5	WT > KO	similar to putative G-protein coupled receptor; predicted gene 2635; component of Sp100-rs; predicted gene 2666; predicted gene 7582; predicted gene 7592; predicted gene 7609
1443239_at	138.6	47	−1.56	2.9	WT > KO	microtubule-associated protein 2
1421916_at	381	144	−1.4	2.6	WT > KO	platelet derived growth factor receptor, alpha polypeptide
1419971_s_at	4010.9	1451.2	−1.47	2.8	WT > KO	solute carrier family 35, member A5
1419972_at	434.2	98	−2.15	4.4	WT > KO	solute carrier family 35, member A5
1448346_at	3281.1	1193.2	−1.46	2.7	WT > KO	cofilin 1, non-muscle; similar to Cofilin-1 (Cofilin, non-muscle isoform); predicted gene 6180
1419021_at	55.1	4.5	−3.61	12	WT > KO	mcf.2 transforming sequence
1434958_at	95.8	35.5	−1.43	2.7	WT > KO	sacsin
1433382_at	217.5	77.5	−1.49	2.8	WT > KO	energy homeostasis associated
1446512_at	214	85.2	−1.33	2.5	WT > KO	predicted gene 5909; zinc finger CCCH-type containing 15
1432298_at	196	68.6	−1.51	2.9	WT > KO	RIKEN cDNA 4921508M14 gene
1446095_at	217.3	53.9	−2.01	4	WT > KO	antisense Igf2r RNA
1445453_at	270.3	91	−1.57	3	WT > KO	helicase with zinc finger domain
1452494_s_at	75.6	29.5	−1.36	2.6	WT > KO	solute carrier organic anion transporter family, member 1b2
1442833_at	837.4	144.8	−2.53	5.8	WT > KO	DNA segment, Chr 15, ERATO Doi 30, expressed
1447049_at	112.7	34.8	−1.7	3.2	WT > KO	IQ motif and WD repeats 1
1441283_at	325.7	112	−1.54	2.9	WT > KO	cyclin Y; similar to cyclin fold protein 1
1434067_at	267.8	78.7	−1.77	3.4	WT > KO	expressed sequence AI662270
1434068_s_at	290.4	49.6	−2.55	5.9	WT > KO	expressed sequence AI662270
1422313_a_at	540.1	213.1	−1.34	2.5	WT > KO	insulin-like growth factor binding protein 5
1449405_at	2035.8	731.6	−1.48	2.8	WT > KO	tensin 1
1425555_at	164.7	45	−1.87	3.7	WT > KO	CDC2-related kinase, arginine/serine-rich
1420073_s_at	176.4	64.8	−1.44	2.7	WT > KO	gb:C78041 EST
1443347_at	99.8	37	−1.43	2.7	WT > KO	gb:BG063775 EST

Table 2 (continued)

ID	WT intensity	KO intensity	log2 (KO/WT)	Fold-change KO vs WT	Diff expr	Gene name
1444498_at	147.3	52.9	−1.48	2.8	WT > KO	gb:BM116117 EST
1444591_at	316.8	71.1	−2.16	4.5	WT > KO	gb:AI429418 EST
1445902_at	139.1	40.7	−1.77	3.4	WT > KO	gb:BG076325 EST
1457122_at	342.7	122.1	−1.49	2.8	WT > KO	gb:BB209527 EST
1458257_at	109.4	40.7	−1.43	2.7	WT > KO	gb:BM196689 EST

shown in (Additional File 1). The enrichment of functional categories phosphoprotein, acetylation, phosphate metabolic process, phosphorus metabolic process and phosphorylation was prominent in both up-regulated and down-regulated genes in U19/EAF2ko vs WT. Notable differences found included enrichment of nucleotide binding, cytoplasm, ATP-binding, death, and apoptosis in up-regulated genes; and alternative splicing, splice variant, nucleus, positive regulation of transcription and gene expression and intracellular signaling cascade in down-regulated genes. One notable gene in the phosphoprotein category was the down-regulated gene Ras and Rab interactor 1 (RIN1). RIN1 is a known RAS effector that has been shown to mediate actin remodeling associated with adhesion and migration of epithelial cells [39]. In this study, knockdown of RIN1 in MCF10A cells enhanced cell migration significantly. Reduced expression of RIN1 in the EAF2 knockout model may also contribute to the disruption of the RAS signaling pathway.

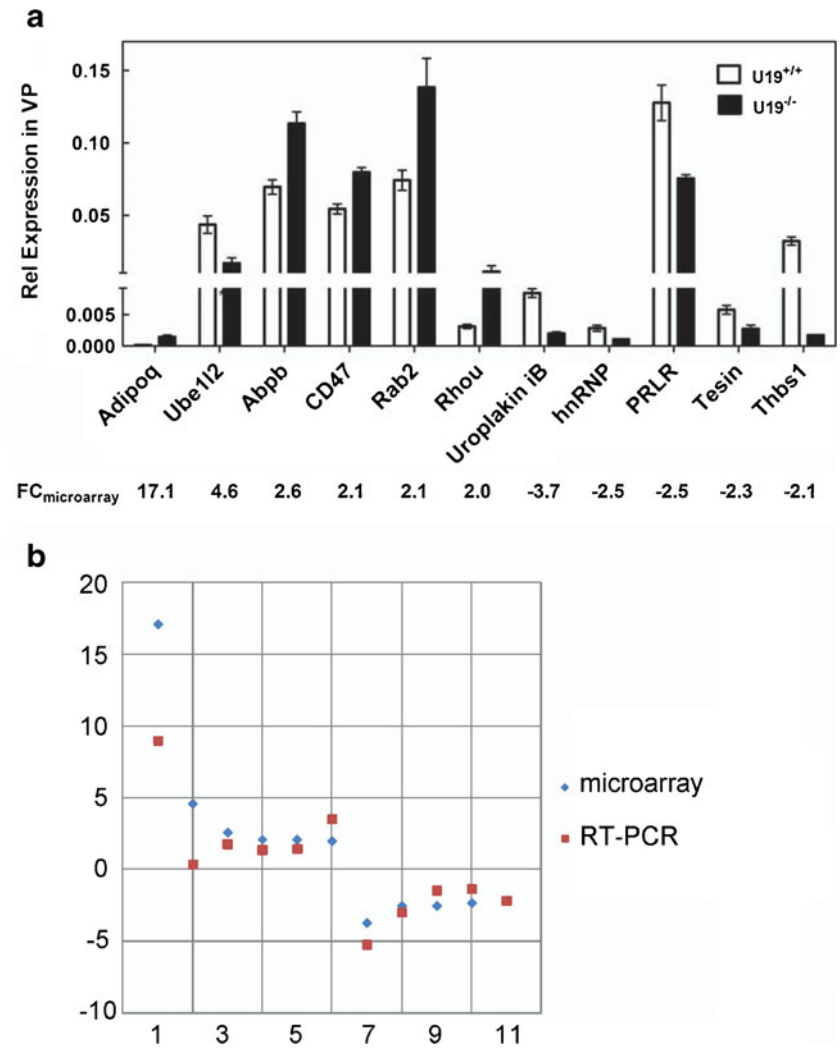

Fig. 2 Concordance of microarray and qPCR gene expression analyses. **a** Bar chart of qPCR data results and corresponding array signals. Data were normalized to GAPDH. **b** Log-fold changes from the microarray platforms are plotted versus the corresponding fold changes from qPCR. R=0.92. Genes 1–11 represent Adipoq, Ube1l2, Abpb, CD47, Rab2, Rhou, Uroplakin iB, hnRNP, Tesin, Thbs1, and PRLR, respectively

Table 3 KEGG pathways identified by DAVID analysis of differentially expressed genes in the U19/EAF2 knockout ventral prostate

Rank	KEGG pathway name	Genes	%	*P*-value
1	Ubiquitin mediated proteolysis	HUWE1, XIAP, CBL, TRIP12, UBA6	3.3	0.02
2	MAPK signaling pathway	BRAF, ACVRIC, PDGFRA, PPP3CB, STK3, ZAK	3.9	0.04
3	Focal adhesion	BRAF, XIAB, COL4A2, CCND2, PDGFRA	3.3	0.06
4	Cell cycle	BUB3, CCND2, STAG1, GM4202	2.6	0.07
5	Pathways in cancer	BRAF, XIAP, ALVRIC, COL4A2, PDGFRA, CBL	3.9	0.09

Up-Regulation of RAS-BRAF Signaling and Phosphorylated ERK in Response to U19/EAF2 Loss

Since U19/EAF2 is a tumor suppressor, we were particularly interested in identifying its downstream genes relevant to carcinogenesis. KEGG pathways identified using DAVID in differentially expressed genes are listed in Table 3. BRAF was listed in three of the identified pathways: MAPK signaling pathway, focal adhesion and pathways in cancer. BRAF (1456505_at) encodes a protein belonging to the raf/mil family of serine/threonine protein kinases and plays a role in regulating the MAPK/ERKs signaling pathway, which affect cell division, differentiation, and secretion. Since BRAF is a key regulator in the RAS and p-ERK signaling pathway and elevated ERK pathway is associated with prostate cancer progression [7, 17–19], we verified BRAF mRNA up-regulation by U19/EAF2 knockout in 3-month old mouse prostate by qPCR (Fig. 3a, *** $p<0.001$). We also tested the effect of U19/EAF2 knockout on BRAF expression in the liver and lung because these two organs developed malignant tumors in U19/EAF2 knockout mice [26]. As expected, BRAF mRNA levels in *U19/EAF2* knockout lung (** $p<0.01$) and liver (* $p<0.05$) (Fig. 3b) were significantly increased compared to wild-type. Elevated p-ERK signal is associated with increased RAS-BRAF cascade signaling. Activation of pathway intermediates such as RAS and BRAF as RAS and BRAF lead to activation of ERK signaling [40–44]. Western Blot analysis showed that total ERK protein levels were not changed in the knockout organs but phosphorylated ERK levels were increased in the ventral prostates and livers of the knockout mice (Fig. 3c), validating the elevated p-ERK level in the knockout prostate and liver (Fig. 3d). Figure 4 summarizes the effects of U19/EAF2 loss on the p-ERK signaling pathway identified by microarray and verified by qPCR and western blot analyses.

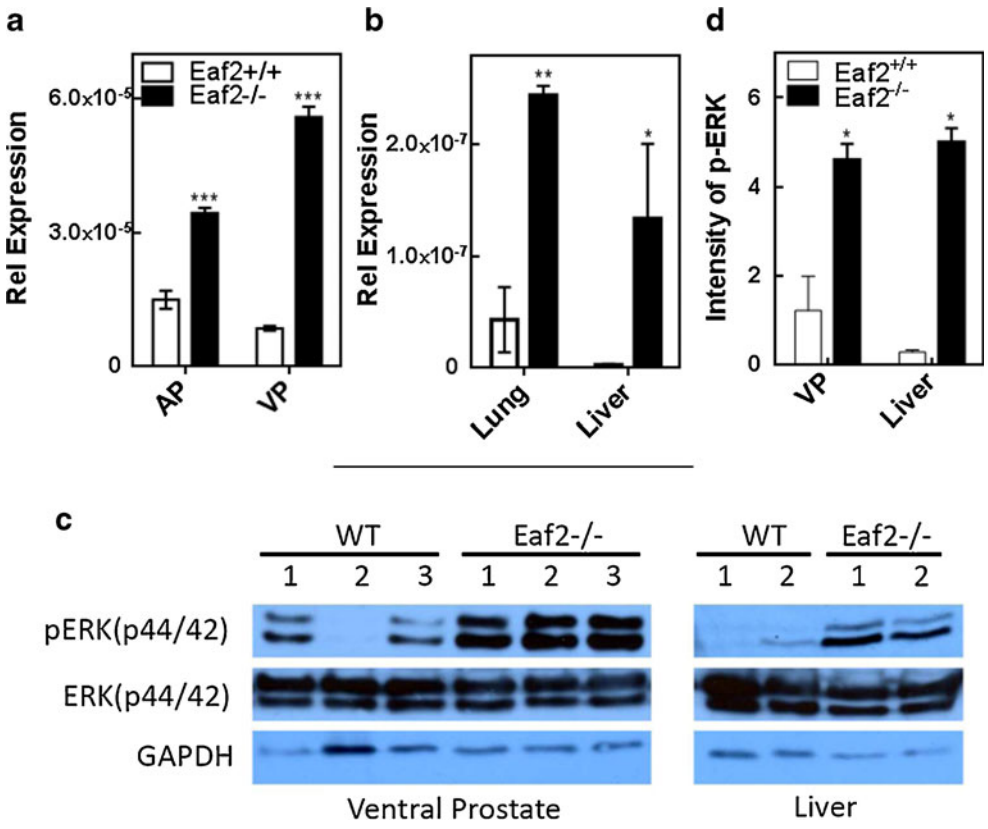

Fig. 3 Effect of *U19/EAF2* knockout on the expression of BRAF mRNA and p-ERK in the mouse model. **a**. qPCR analysis of the BRAF mRNA levels in anterior prostate (AP) and ventral prostate (VP) and **b**. lung and liver of *U19/EAF2* knockout and wild-type control mice.. Data were normalized to GAPDH, ($n=3$). **c**. Western blot analysis of phosphorylated ERK, pERK(p44/42), in *U19/EAF2* knockout and wild-type mouse tissues. Images shown are representative blots for ERK, pERK and GAPDH from ventral prostates and liver lysates of individual *U19/EAF2* knockout and wild-type control mice. **d**. Intensity of p-ERK in / EAF2 knockout and wild-type mouse tissues. Band densities in the Western blots were analyzed with IMAGEJ (National Institutes of Health) and normalized against GAPDH. Data represent the mean ± SEM; * $p<0.05$. ** $p<0.01$, *** $p<0.001$ versus WT

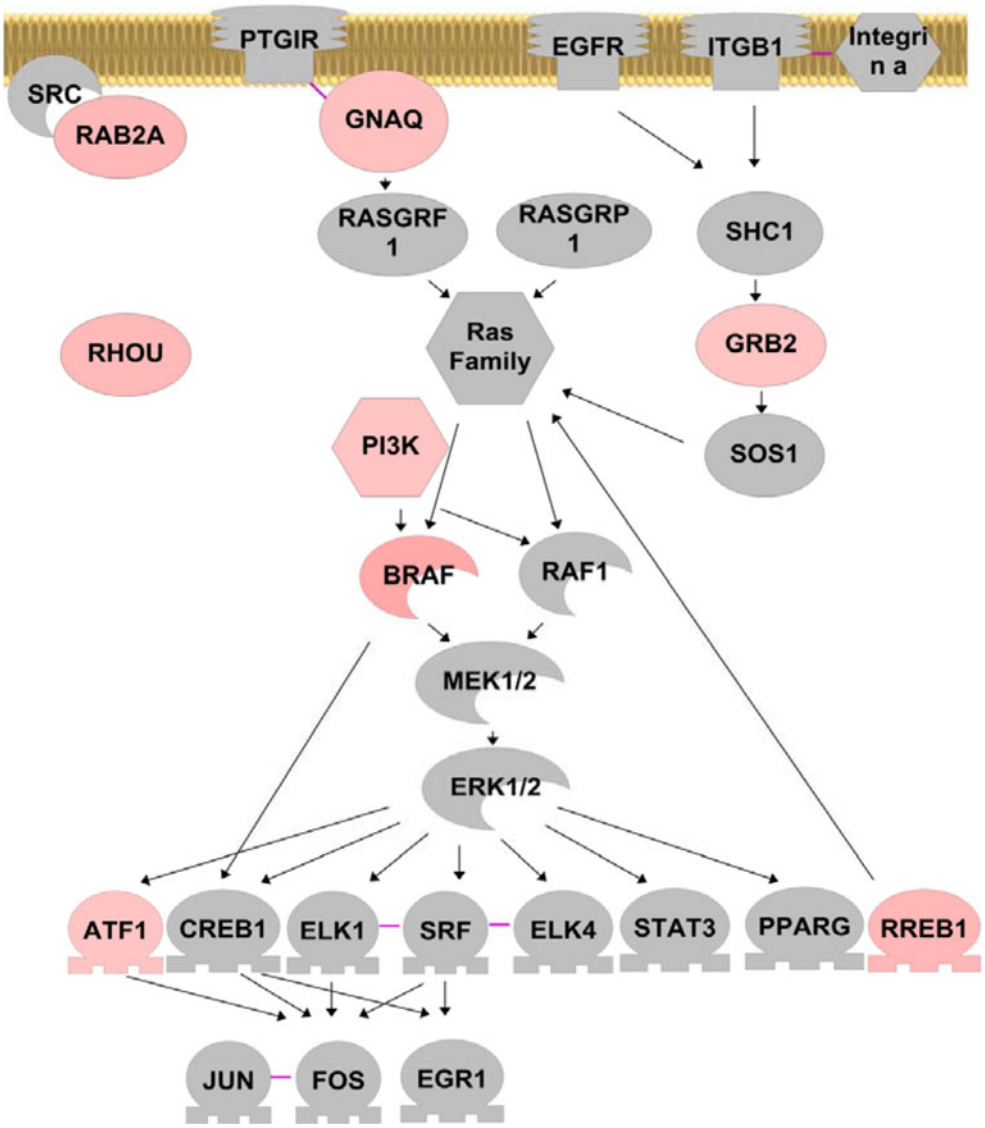

Fig. 4 Effect of *U19/EAF2* knockout on ERK pathway in the murine prostate. Genes up-regulated upon U19/EAF2 knockout are colored in peach. Color intensity is used to indicate the degree of up-regulation, with light peach color for less up-regulation and darker peach color for more up-regulation. Solid arrows indicate positive regulation; solid purple lines indicate protein binding

Discussion

Androgens play an important role in maintaining prostate homeostasis [45, 46]. Disruption of prostatic homeostasis may lead to abnormal prostate growth and/or carcinogenesis. However, the mechanisms of androgen-regulated prostatic homeostasis are poorly understood. U19/EAF2 represents one important androgen-responsive gene involved in prostate homeostasis, because U19/EAF2 knockout prostate exhibited elevated cell proliferation [26]. U19/EAF2 also plays an important role in the regulation of TSP1 [47]. TSP-1 expression is inhibited in a large number of tumors, including breast and androgen-dependent prostate carcinomas in which there is an inverse correlation between TSP1 expression and microvessel density [48–50]. In addition to the increased incidence in mPIN lesions, the EAF2 knockout mouse prostate is also characterized by increased microvessel density and stromal inflammation [51]. These studies suggest that EAF2 loss impacts not only epithelial cell proliferation but also the surrounding stroma and vasculature. Identification of pathways regulated by U19/EAF2 using cDNA microarray provides mechanistic insights into U19/EAF2 action as well as androgen action in the prostate microenvironment.

Bioinformatics analysis using DAVID software revealed multiple pathways associated with and potential disease relevance of genes that are differentially regulated in U19/EAF2 knockout prostate (Additional File 1, Table 3). Many of the U19/EAF2 downstream genes are involved in mRNA transcription and mRNA transcription regulation, suggesting that U19/EAF2 can regulate mRNA transcription directly as a transcription factor and/or a transcription elongation factor as well as indirectly through up- or down-regulating genes capable of modulating transcription. U19/EAF2 modulation of mRNA transcription is supported by the identification of more than 100 differentially-regulated mRNA transcripts. Identification of genes involved in protein phosphorylation and modification as

well as proteolysis suggests a role for U19/EAF2 in the regulation of various signaling pathways at the protein levels, which was substantiated by the elevated phosphorylation of ERK in the U19/EAF2 knockout prostate (Fig. 3). Interestingly, U19/EAF2 knockout also affects genes involved in the metabolism of nucleoside, nucleotide, and nucleic acid, suggesting a potential role for U19/EAF2 in the regulation of metabolism. The above observations provided evidence for U19/EAF2 regulation of biological processes at levels of mRNA, protein and metabolism.

According to KEGG pathway analysis, the biological processes affected by U19/EAF2 knockout are most relevant to cancer, reproductive system diseases, cell death, and cell cycle (Additional File 1, Table 3). This finding is consistent with the observation that U19/EAF2 knockout mouse exhibited tumor development in multiple organs, defects in reproductive systems including testes and the prostate, elevated cell death in testes, and elevated cell proliferation in the prostate [26, 52]. Toxicity analysis revealed the relevance of U19/EAF2 downstream genes with diseases in the liver and heart multiple times, which again agrees with the phenotypes observed in the U19/EAF2 knockout mice, particularly hepatocellular carcinoma, elevated angiogenesis in the liver and heart enlargement. The identification of U19/EAF2 downstream genes will provide a strong foundation to explore the molecular mechanisms underlining various phenotypes caused by U19/EAF2 knockout.

As a potential transcription factor/transcription elongation factor regulated by androgens, U19/EAF2 may mediate androgen-induced expression of some androgen-responsive genes. A search for androgen responsive genes [53] identified 2 androgen-responsive genes differentially expressed in U19/EAF2 knockout prostate. X-linked inhibitor of apoptosis (XIAP), which was identified by KEGG pathway analysis in ubiquitin mediated proteolysis, focal adhesion and pathways in cancer, was up-regulated 3.1-fold in U19/EAF2 knockout prostate. XIAP is down-regulated by androgens in normal prostate epithelial cells [54]. Serine/threonine kinase 3 (STK3), was up-regulated 2.5-fold in U19/EAF2 knockout prostate. STK3 is a MAPK signaling pathway gene that is up-regulated in response to androgens in human breast cancer cells [55]. These observations suggest a role for U19/EAF2 in mediating androgen regulation of gene expression in the prostate. Since U19/EAF2 is a putative DNA-binding transcription factor, its regulation of downstream genes may involve direct binding of U19/EAF2 to the promoter/enhance regions of these targeted genes. However, it is also possible that U19/EAF2 can enhance transcription elongation. Further studies will be required to determine the mechanism by which U19/EAF2 controls the expression of its downstream genes.

Identification of the RAS-BRAF-MEK-ERK cascade as a downstream target of U19/EAF2 in the prostate provides new insights into the mechanism associate with tumorigenesis in U19/EAF2 knockout mice (Fig. 4). Multiple genes, GRB2, PI3K, RHOU, RAB2, BRAF and RREB-1, were up-regulated in U19/EAF2 knockout prostate, suggesting coordinated regulation of this important pathway by U19/EAF2. Elevated phosphorylation of ERK in the U19/EAF2 knockout prostate confirmed the activation of RAS-BRAF-MEK-ERK signaling upon U19/EAF2 deletion. The activation of this pathway was not limited to the prostate, because ERK phosphorylation was also significantly enhanced in the liver of U19/EAF2 knockout mice (Fig. 3). Since abnormal activation of RAS-BRAF-MEK-ERK is often associated with and functionally important in tumorigenesis, activation of this pathway is likely a key step leading to tumorigenesis in U19/EAF2 knockout mice.

In summary, this study revealed multiple pathways regulated by U19/EAF2 in the prostate and identified RAS-BRAF-MEK-ERK pathway as a downstream target of U19/EAF2. Bioinformatic analysis of U19/EAF2 downstream genes showed the functional relevance of U19/EAF2 regulated pathways with cancer, liver diseases, cardiac abnormality, and defects in reproductive system, which was observed in U19/EAF2 knockout mice [26, 52]. These observations argue that these U19/EAF2 downstream pathways are likely mediating U19/EAF2 function in vivo, with the RAS-BRAF-MEK-ERK signaling as a potential key mediator of U19/EAF2 knockout induced tumorigenesis.

Acknowledgement This study was supported in part by National Institutes of Health Grants R37 DK51193, R01 CA 108675, and P50 CA90386 and the Tippins Foundation (LEP). This project used the UPCI Animal Facility and was supported in part by award P30CA047904. We also thank Junkui Ai and Liquan Cai for critical reading.

Disclosure Summary The authors have nothing to disclose.

References

1. Kozlowski JM, Ellis WJ, Grayhack JT (1991) Advanced prostatic carcinoma. Early versus late endocrine therapy. Urol Clin N Am 18 (1):15–24
2. Montie J, Pienta K (1994) Review of the role of androgenic hormones in the epidemiology of benign prostatic hyperplasia and prostate cancer. [Review]. Urology 43(6):892–899
3. O'Leary MP, Roehrborn CG, Black L (2007) Dutasteride significantly improves quality of life measures in patients with enlarged prostate. Prostate Cancer Prostatic Dis
4. Griffiths K, Eaton C, Harper M, Peeling B, Davies P (1991) Steroid hormones and the pathogenesis of benign prostatic hyperplasia. [Review]. Eur Urol 20(Suppl 1):68–77
5. Zhou Z, Wong C, Sar M, Wilson E (1994) The androgen receptor: an overview. [Review]. Recent Prog Horm Res 49:249–274
6. Wang Z, Tufts R, Haleem R, Cai X (1997) Genes regulated by androgen in the rat ventral prostate. Proc Natl Acad Sci USA 94:12999–13004
7. Zhu ML, Kyprianou N (2008) Androgen receptor and growth factor signaling cross-talk in prostate cancer cells. Endocr Relat Cancer 15(4):841–849

8. Culig Z (2004) Androgen receptor cross-talk with cell signalling pathways. Growth Factors 22(3):179–184
9. Maurer G, Tarkowski B, Baccarini M (2011) Raf kinases in cancer-roles and therapeutic opportunities. Oncogene 30(32):3477–3488
10. Marais R, Light Y, Paterson HF, Mason CS, Marshall CJ (1997) Differential regulation of Raf-1, A-Raf, and B-Raf by oncogenic ras and tyrosine kinases. J Biol Chem 272(7):4378–4383
11. Niihori T, Aoki Y, Narumi Y, Neri G, Cave H, Verloes A, Okamoto N, Hennekam RC, Gillessen-Kaesbach G, Wieczorek D et al (2006) Germline KRAS and BRAF mutations in cardio-facio-cutaneous syndrome. Nat Genet 38(3):294–296
12. Tabernero J, Dienstmann R (2011) BRAF as a target for cancer therapy. Anti-Cancer Agent Me 11(3):285–295
13. Davies H, Bignell GR, Cox C, Stephens P, Edkins S, Clegg S, Teague J, Woffendin H, Garnett MJ, Bottomley W et al (2002) Mutations of the BRAF gene in human cancer. Nature 417(6892):949–954
14. Halilovic E, Solit DB (2008) Therapeutic strategies for inhibiting oncogenic BRAF signaling. Curr Opin Pharmacol 8(4):419–426
15. Pratilas CA, Xing F, Solit DB (2011) Targeting oncogenic BRAF in human cancer. Curr Top Microbiol Immunol
16. Ball DW, Jin N, Rosen DM, Dackiw A, Sidransky D, Xing M, Nelkin BD (2007) Selective growth inhibition in BRAF mutant thyroid cancer by the mitogen-activated protein kinase kinase 1/2 inhibitor AZD6244. J Clin Endocrinol Metab 92(12):4712–4718
17. Gioeli D, Mandell JW, Petroni GR, Frierson HF Jr, Weber MJ (1999) Activation of mitogen-activated protein kinase associated with prostate cancer progression. Cancer Res 59(2):279–284
18. Gioeli D (2005) Signal transduction in prostate cancer progression. Clin Sci (Lond) 108(4):293–308
19. Garraway LA, Thomas RK, Baker AC, DeBiasi RM, Winckler W, LaFramboise T, Lin WM, Wang M, Feng W, Zander T et al (2007) High-throughput oncogene mutation profiling in human cancer. Nat Genet 39(3):347–351
20. Barford D, Wan PTC, Garnett MJ, Roe SM, Lee S, Niculescu-Duvaz D, Good VM, Jones CM, Marshall CJ, Springer CJ et al (2004) Mechanism of activation of the RAF-ERK signaling pathway by oncogenic mutations of B-RAF. Cell 116(6):855–867
21. Dahut WL, Scripture C, Posadas E, Jain L, Gulley JL, Arlen PM, Wright JJ, Yu Y, Cao L, Steinberg SM et al (2008) A phase II clinical trial of sorafenib in androgen-independent prostate cancer. Clin Cancer Res 14(1):209–214
22. Xiao W, Zhang Q, Jiang F, Pins M, Kozlowski JM, Wang Z (2003) Suppression of prostate tumor growth by U19, a novel testosterone-regulated apoptosis inducer. Cancer Res 63(15):4698–4704
23. Simone F, Luo RT, Polak PE, Kaberlein JJ, Thirman MJ (2003) ELL-associated factor 2 (EAF2), a functional homolog of EAF1 with alternative ELL binding properties. Blood 101(6):2355–2362
24. Xiao W, Jiang F, Wang Z (2006) ELL binding regulates U19/Eaf2 intracellular localization, stability, and transactivation. Prostate 66 (1):1–12
25. Shilatifard A, Duan DR, Haque D, Florence C, Schubach WH, Conaway JW, Conaway RC (1997) ELL2, a new member of an ELL family of RNA polymerase II elongation factors. Proc Natl Acad Sci U S A 94(8):3639–3643
26. Xiao W, Zhang Q, Habermacher G, Yang X, Zhang AY, Cai X, Hahn J, Liu J, Pins M, Doglio L et al (2008) U19/Eaf2 knockout causes lung adenocarcinoma, B-cell lymphoma, hepatocellular carcinoma and prostatic intraepithelial neoplasia. Oncogene 27 (11):1536–1544
27. Cortez DA, Tonon AP, Colepicolo P, Vencio RZ (2011) Combining *P* values to improve classification of differential gene expression in the HTself software. Genetics and Molecular Research: GMR 10 (4):3586–3595
28. Pascal LE, Vencio RZ, Page LS, Liebeskind ES, Shadle CP, Troisch P, Marzolf B, True LD, Hood LE, Liu AY (2009) Gene expression relationship between prostate cancer cells of Gleason 3, 4 and normal epithelial cells as revealed by cell type-specific transcriptomes. BMC Cancer 9:452
29. Pascal LE, Goo YA, Vencio RZ, Page LS, Chambers AA, Liebeskind ES, Takayama TK, True LD, Liu AY (2009) Gene expression down-regulation in CD90+ prostate tumor-associated stromal cells involves potential organ-specific genes. BMC Cancer 9:317
30. Pascal LE, Vencio RZ, Vessella RL, Ware CB, Vencio EF, Denyer G, Liu AY (2011) Lineage relationship of prostate cancer cell types based on gene expression. BMC Medical Genomics 4:46
31. da Huang W, Sherman BT, Lempicki RA (2009) Systematic and integrative analysis of large gene lists using DAVID bioinformatics resources. Nat Protoc 4(1):44–57
32. Dennis G Jr, Sherman BT, Hosack DA, Yang J, Gao W, Lane HC, Lempicki RA (2003) DAVID: Database for annotation, visualization, and integrated discovery. Genome Biol 4(5):P3
33. Ai J, Wang Y, Dar JA, Liu J, Liu L, Nelson JB, Wang Z (2009) HDAC6 regulates androgen receptor hypersensitivity and nuclear localization via modulating Hsp90 acetylation in castration-resistant prostate cancer. Mol Endocrinol 23(12):1963–1972
34. Shi Q, Pavey ES, Carter RE (2012) Bonferroni-based correction factor for multiple, correlated endpoints. Pharm Stat 11(4):300–309
35. Bridges LC, Tani PH, Hanson KR, Roberts CM, Judkins MB, Bowditch RD (2002) The lymphocyte metalloprotease MDC-L (ADAM 28) is a ligand for the integrin alpha4beta1. J Biol Chem 277(5):3784–3792
36. Crawford NP, Alsarraj J, Lukes L, Walker RC, Officewala JS, Yang HH, Lee MP, Ozato K, Hunter KW (2008) Bromodomain 4 activation predicts breast cancer survival. Proc Natl Acad Sci U S A 105(17):6380–6385
37. Busch C, Hanssen TA, Wagener C (2002) B OB: Down-regulation of CEACAM1 in human prostate cancer: correlation with loss of cell polarity, increased proliferation rate, and Gleason grade 3 to 4 transition. Hum Pathol 33(3):290–298
38. van der Rest M, Garrone R (1991) Collagen family of proteins. FASEB J: Off Publ Fed Am Soc Exp Biol 5(13):2814–2823
39. Hu H, Bliss JM, Wang Y, Colicelli J (2005) RIN1 is an ABL tyrosine kinase activator and a regulator of epithelial-cell adhesion and migration. Current biology: CB 15(9):815–823
40. Lewis TS, Shapiro PS, Ahn NG (1998) Signal transduction through MAP kinase cascades. Adv Cancer Res 74:49–139
41. Cobb MH, Goldsmith EJ (1995) How map kinases are regulated. J Biol Chem 270(25):14843–14846
42. Hynes NE, Lane HA (2005) ERBB receptors and cancer: the complexity of targeted inhibitors. Nat Rev Cancer 5(5):341–354
43. Allen LF, Sebolt-Leopold J, Meyer MB (2003) Cl-1040 (PD184352), a targeted signal transduction inhibitor of MEK (MAPKK). Semin Oncol 30(5):105–116
44. Pratilas CA, Taylor BS, Ye Q, Viale A, Sander C, Solit DB, Rosen N (2009) (V600E)BRAF is associated with disabled feedback inhibition of RAF-MEK signaling and elevated transcriptional output of the pathway. Proc Natl Acad Sci U S A 106(11):4519–4524
45. Bruchovsky N, Lesser B, Doorn EV, Craven S (1975) Hormonal effects on cell proliferation in rat prostate. Vitam Horm 33:61–102
46. Isaacs J, Furuya Y, Berges R (1994) The role of androgen in the regulation of programmed cell death/apoptosis in normal and malignant prostatic tissue. [Review]. Sem Cancer Biol 5(5):391–400
47. Su F, Pascal LE, Xiao W, Wang Z (2010) Tumor suppressor U19/EAF2 regulates thrombospondin-1 expression via p53. Oncogene 29(3):421–431
48. Colombel M, Filleur S, Fournier P, Merle C, Guglielmi J, Courtin A, Degeorges A, Serre CM, Bouvier R, Clezardin P et al (2005) Androgens repress the expression of the angiogenesis inhibitor

thrombospondin-1 in normal and neoplastic prostate. Cancer Res 65 (1):300–308
49. Fontana A, Filleur S, Guglielmi J, Frappart L, Bruno-Bossio G, Boissier S, Cabon F, Clezardin P (2005) Human breast tumors override the antiangiogenic effect of stromal thrombospondin-1 in vivo. Int J Cancer J Int Du Cancer 116(5):686–691
50. Kwak C, Jin RJ, Lee C, Park MS, Lee SE (2002) Thrombospondin-1, vascular endothelial growth factor expression and their relationship with p53 status in prostate cancer and benign prostatic hyperplasia. BJU Int 89(3):303–309
51. Pascal LE, Ai J, Rigatti LH, Lipton AK, Xiao W, Gnarra JR, Wang Z (2011) EAF2 loss enhances angiogenic effects of Von Hippel-Lindau heterozygosity on the murine liver and prostate. Angiogenesis 14 (3):331–343
52. Xiao W, Ai J, Habermacher G, Volpert O, Yang X, Zhang AY, Hahn J, Cai X, Wang Z (2009) U19/Eaf2 binds to and stabilizes von hippel-lindau protein. Cancer Res 69(6):2599–2606
53. Jiang M, Ma Y, Chen C, Fu X, Yang S, Li X, Yu G, Mao Y, Xie Y, Li Y (2009) Androgen-responsive gene database: integrated knowledge on androgen-responsive genes. Mol Endocrinol 23(11):1927–1933
54. Long RM, Morrissey C, Walsh S, Hamilton HJ, Farrell N, O'Neill A, Fitzpatrick JM, Watson WR (2007) Alterations in the expression of inhibitors of apoptosis during differentiation of prostate epithelial cells. BJU Int 100(2):445–449
55. Doane AS, Danso M, Lal P, Donaton M, Zhang L, Hudis C, Gerald WL (2006) An estrogen receptor-negative breast cancer subset characterized by a hormonally regulated transcriptional program and response to androgen. Oncogene 25(28):3994–4008